Preliminary Study of a Dual PMT Lithium-Cadmium Hybrid Neutron Detector

Trevor Jex

A senior thesis submitted to the faculty of
Brigham Young University
in partial fulfillment of the requirements for the degree of

Bachelor of Science

Lawrence Rees, Advisor

Department of Physics and Astronomy

Brigham Young University

April 2014

ABSTRACT

Preliminary Study of a Dual PMT Lithium-Cadmium Hybrid Neutron Detector

Trevor Jex
Department of Physics and Astronomy
Bachelor of Science

Neutron detection is an important component to Homeland Security. Portal monitors are put at points of entry into the country to detect illegal nuclear material entering the United States. In the past and currently, ^{3}He-based detectors have and are being used in these portals. However, because of the current shortage of ^{3}He, the BYU Nuclear Group is looking for alternative methods for neutron detection. In particular, I have been doing preliminary work on a two-photomultiplier tube hybrid neutron detector that utilizes lithium and cadmium components. This work focuses on how each component of the hybrid (lithium and cadmium) performs on its own. It then outlines what results are seen when both sides are simultaneously "watching" the same radiation source. Both the cadmium and lithium components work as expected when operating alone. When combined– i.e. both components are on and looking at the same radiation source–we see that the cadmium component is the dominating detection component in the hybrid detector. Relatively few events are seen from the lithium side. Further work should be done to confirm the results herein, to consider other setups that may yield more balanced results as well as to confirm the hope that a hybrid detector, such as the one here, can detect neutrons over a broader energy range than either component by itself. If this can be accomplished, the hybrid detector will become a more viable candidate for potential use in homeland security.

Keywords: neutron, neutron detection, cadmium, lithium, pulse shape discrimination, PSD, dual pulses, doubles

ACKNOWLEDGMENTS

I would like to thank Dr. Rees for his mentoring and help on this thesis and during my entire time as a member of the BYU Nuclear Group, as well as for taking me on as a member of the group in the first place. This work would not be possible with out his mentoring, teaching and patience.

Thanks to Dr. Czirr for his help on this work and for helping me better understand some of the physics behind neutron detection.

Thanks to Kent Talbert for the help in allowing me to use your data analysis code as well as all other help!

Thank you to the BYU Nuclear Group for their mentoring, help and friendship.

A big thanks to all friends, family, study groups, fellow physics students and everyone who helped me make it to this point.

A special thanks to my wife, Amanda and daughter, Miriam, who have stuck with me both through these past few busy weeks as well as throughout my entire time here in BYU Physics. I love you both!

Parts of this work were funded by NNSA Grant no. DE-FG52-10NA29655 and DHS Award no. 2010-DN-077-ARI039-02.

Contents

Chapter 1

Introduction

1.1 Introduction to Neutron Detection

Neutron detection is, as its name suggests, the process of finding new and improved methods for detecting neutrons. As a subfield of nuclear physics, neutron detection has a broad range of applications. Apart from the physicist's quest to gain further scientific understanding–whether theoretical, experimental or both–in all aspects of physics, neutron detection is important in the field of Homeland Security [1–5]. In this arena, current solutions to the question of neutron detection face certain challenges [1, 2, 4, 5]. In response to these challenges, the BYU Nuclear Group has engaged itself to find new answers to the question of neutron detection.

The obvious yet still-illusive challenge of neutron detection is the nature of the neutron itself–a particle with no charge. As such, the whole thrust of neutron detection currently relies on the indirect detection of this neutral particle. Since we cannot see nor detect the neutron directly, we use subatomic interactions, such as neutron collisions with hydrogen nuclei, for detection. Because the method of detection is indirect, the main challenge is thus realized: "Are the interactions we see the result of neutrons or some other particle/force?" The key to successful neutron detection

becomes not only the ability to "see" the indirect results of neutron interactions, but to successfully distinguish between the interactions triggered by a neutron and those triggered by some other means.

Timeliness and accuracy are foundational to real-life neutron detection and both incur challenges to overall detector system construction and implementation [3, 6]. The largest real-life application of neutron detection, at least as concerns the BYU Nuclear Group, is Homeland Security. In response to the ever-present possibility of a nuclear attack against the U.S., the Department of Homeland Security (DHS) is using the technology of neutron detection at border-crossings, seaports and airports to aid in the detection of illicit nuclear material crossing into US territory [1–3].

Up to the present, neutron detection by DHS has relied heavily on the abilities (and availability) of helium-3 (^{3}He) [1, 2, 4, 5]. ^{3}He has an excellent thermal neutron cross-section (5330 barns [7]), meaning it has the desired characteristics to regularly interact with neutrons as compared to other materials that may not interact with neutrons as regularly. The principle limitation of ^{3}He is not its capability to interact with neutrons, but rather something much less scientific: its shortage [1,2,4,5]. ^{3}He is harvested as the by-product of the tritium used in nuclear warheads. In a research report to congress, Morgan and Shea described the situation:

> "Over time, tritium decays into helium-3 and must be replaced to maintain warhead effectiveness. The NNSA recycles the mixture of tritium and helium-3 that results from this decay process and reuses the resulting pure tritium. From the perspective of the weapons program, the extracted helium-3 is a byproduct of maintaining the purity of the tritium supply. This means that the tritium needs of the weapons program, not the demand for helium-3 itself, determine the amount of helium-3 produced." [1]

^{3}He's greatest strengths shine in its ability to detect neutrons at relatively low energies, its ability to "discriminate" well between neutrons and gamma rays, and the simplicity of the detection system it is integrated into. However, because of shortage, there is a need for alternatives to ^{3}He [2].

In response to this need, the BYU Nuclear Group is working to design and test detectors that provide a viable alternative to ^{3}He detectors–always keeping in mind the need for accurate neutron/gamma discrimination as well as acceptable overall detector efficiency. The Nuclear Group's focus is mainly cadmium-based and lithium-based detectors. In particular, I have been doing work on a "hybrid" of these two components. The purpose of the "hybrid" detector is to see if and how the structure of a cadmium detector component aids a lithium component and vice versa. The for this setup is that the abilities of these two "separate" detectors when combined into one assembly, provide a "single" detector that can adequately discriminate between neutrons and gammas as well as detect neutrons over a broad energy range: broader than either component separately.

The remainder of this work covers the basics of neutron-detection physics, results for the Nuclear Group's cadmium-based and lithium-based detectors thus far, premise and motivation for the hybrid detector, experimental setup for the hybrid and finally, the results from the hybrid and the conclusions drawn as a result.

Chapter 2

Neutron Detection: Basic Physics

The physics involved in basic neutron detection can be broken down into three parts: (1) the interactions of subatomic particles, (2) the conversion of these interactions into light and (3) the transformation of these light pulses into an electrical signal to be read into a digitizer and computer.

2.1 Interactions on the Subatomic Scale

Because neutrons are not charged particles, we are currently limited to detecting them indirectly, i.e. observing the behavior of charged particles that have interacted with neutrons. In essence, we watch the behavior of protons and nuclei when they come into contact with a neutron. (Note: Gamma ray interactions can produce similar behaviors.) Depending on the type of behavior exhibited, we can detect the subatomic interaction and then possibly decipher its origin with either a neutron or gamma ray.

Before going over the physics of the interactions, I will briefly review the types of interactions that are likely to occur during the experiment. First, there is the collision of a neutron with a proton. Next there is the possibility of a neutron at lower energy being captured; this will result in a nucleus at a higher energy state that must somehow de-excite. Last, I will go over the Compton

effect–the scattering of gamma rays from electrons.

2.1.1 Neutron-Proton Collisions

When colliding with one another (at least in the energy realm we are dealing with in neutron detection), neutrons and protons must scatter elastically. In an elastic collision, when one particle collides with the other, any kinetic energy being transferred from the first particle goes directly into kinetic energy for the second particle. An example of this is seen when a moving ping-pong ball of mass m_p, travelling with velocity v_1, collides with a stationary ping-pong ball, also of mass m_p. In this case, using conservation of energy, any kinetic energy transfer from the first ball to the second will remain in the form of kinetic energy for the second. Also, using conservation of momentum, we know that the momentum of the first ball, p_1 (which includes direction, say along the +x-axis), must be conserved. Two different situations below, with accompanying figures, illustrate the process of elastic collision.

Situation 1: Ping-pong ball 1 transfers all of its kinetic energy to ping-pong ball 2, which "utilizes" all this new energy as kinetic energy. This situation (shown in Fig. 2.1 below) can be described using conservation of energy and momentum:

$$\frac{1}{2}m_p v_1^2 = \frac{1}{2}m_p v_2^2 \tag{2.1}$$

$$where \;\; v_1 = v_2$$

$$m_p v_1 = m_p v_2 \tag{2.2}$$

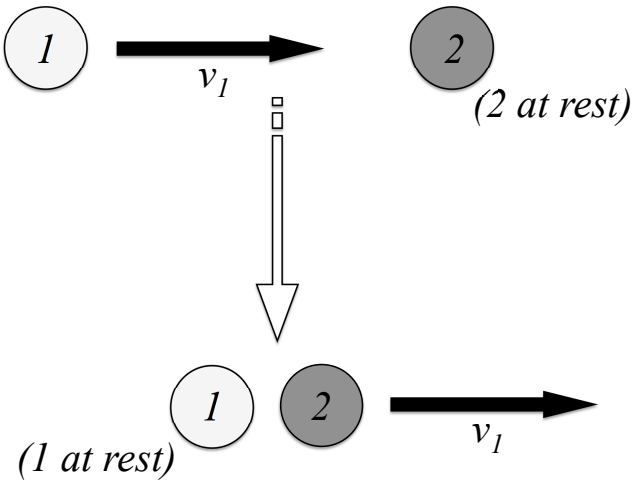

Figure 2.1 Collision of two ping-pong balls where ball 1 transfers all of its kinetic energy to ball 2.

Situation 2: Ping-pong ball 1 transfers only a portion of its kinetic energy to ping-pong ball 2, which "utilizes" all this new energy as kinetic energy. The result for this interaction is that their sum kinetic energies are equal to the original kinetic energy of ball 1. Additionally, the sum of their final momenta is also equal to the initial momentum of ball 1. As before, this situation is described using conservation of energy and conservation of momentum (see Fig. 2.2 below):

$$\frac{1}{2}m_p v_{1_0}^2 = \frac{1}{2}m_p v_{1_f}^2 + \frac{1}{2}m_p v_{2_f}^2 \tag{2.3}$$

$$m_p v_{1_0} = m_p v_{1_f}\cos(\theta_1) + m_p v_{2_f}\cos(\theta_2) \tag{2.4}$$

$$m_p v_{1_f}\sin(\theta_1) + m_p v_{2_f}\sin(\theta_2) = 0 \tag{2.5}$$

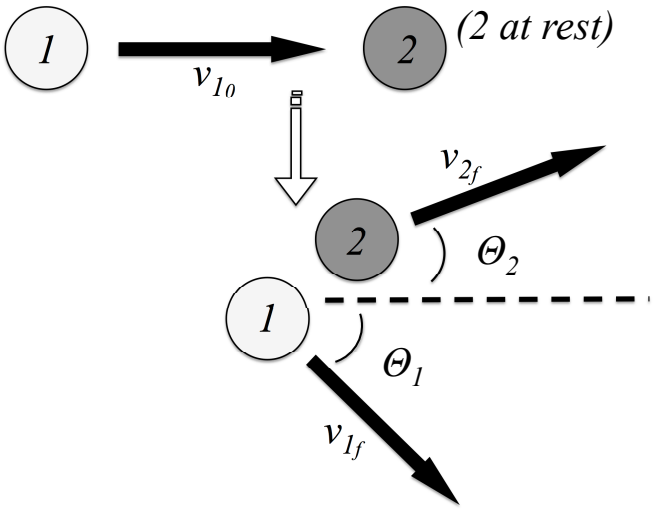

Figure 2.2 Collision of two ping-pong balls where ball 1 transfers only part of its kinetic energy to ball 2.

The same understanding and principle discussed here can be applied to the elastic collisions between protons and neutrons. The following describes an elastic interaction, as given by Knoll [7] in the laboratory reference frame. (I have taken Knoll's version and specified it for the instance of a proton as the recoil nucleus.)

$$E_r = \frac{4A}{(1+A)^2}\cos^2(\theta)E_n \tag{2.6}$$

- E_r = proton energy
- θ = proton scattering angle
- A = proton/neutron mass ratio
- E_n = incident neutron energy

2.1.2 Neutron Capture in ^{113}Cd and ^{6}Li

Once a neutron has slowed down to low enough energy (most likely by elastic collisions with protons) and is in close proximity to a ^{113}Cd or ^{6}Li nucleus (we will focus on these two nuclei as they constitute the main components of the detectors used in the BYU Nuclear Group), it has the potential of being captured by that nucleus. In this capture process, the lone neutron is joined into the capturing nucleus, which then adds excitation energy to the nucleus. The newly excited nucleus, as a result of the capture, is at a higher energy level and must de-excite. In the (n,^{113}Cd) capture reaction, this is done by emission of a cascade of gamma rays from the nucleus. There is around 9MeV energy released for the cascade as a whole and about an average of 1MeV for each gamma ray. In ^{6}Li, the de-excitation occurs via fission of the newly formed ^{7}Li atom into an alpha particle and triton (^{3}H nucleus). The process of capture and de-excitation of the respective nuclei is seen in the following reactions:

$$ {}^{1}_{0}n + {}^{113}Cd \rightarrow {}^{114}Cd^{*} \rightarrow {}^{114}Cd + \gamma \tag{2.7} $$

$$ {}^{1}_{0}n + {}^{6}Li \rightarrow {}^{4}_{2}\alpha + {}^{3}_{1}H \tag{2.8} $$

Where * = Cd in an excited state

Note that both the alpha particle and triton in the second reaction are charged particles. This becomes important subsequently when discussing scintillation.

2.1.3 The Compton effect

The Compton effect, discovered by Arthur Compton [8], describes the interaction of photons and electrons. When a photon (a gamma ray in our case) scatters from an electron, it transfers a portion of its momentum to the electron. This causes the electron to ricochet off in one direction and the

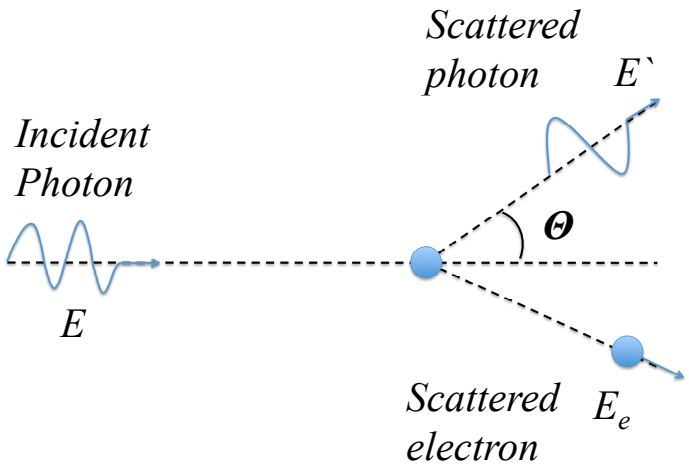

Figure 2.3 A photon scatters off an electron in a process known as Compton scattering.

photon, now at a lower energy and longer wavelength, in another. This is known as Compton scattering. An example of this, based off Krane's depiction [8], is shown above in Fig. 2.3.

The post-impact energy of the photon is related to its pre-impact energy by the angles noted above. Using Krane's derivation and notation we have:

$$\frac{1}{E'} - \frac{1}{E} = \frac{1}{m_e c^2}(1 - \cos\theta) \tag{2.9}$$

Where E' is the post-impact energy of the photon and E is the pre-impact energy.

We can also relate the pre- and post-impact energy of the photon to the resultant energy of the electron by conservation of relativistic energy (based off Krane's notation and derivation):

$$E_e = E + m_e c^2 - E' \tag{2.10}$$

As it relates to neutron detection, it is important to understand that gamma rays can "strip" off

electrons from materials that make up the detector, resulting in the presence of charged particles, such as electrons, in the detector's scintillating material. The presence of charged particles (electrons, alphas, tritons or protons) are what cause the occurrence of light pulses in the scintillator that are then detected by the photomultiplier tube (PMT).

2.2 Scintillation: Converting Subatomic Interactions into Light

The process by which we convert the interaction of charged particles within a specific scintillating material into light pulses is called scintillation. Scintillation occurs differently in the cadmium component of the detector–which contains slabs of scintillating plastic–vs. the lithium glass component. As such, I will briefly discuss each process separately.

2.2.1 Scintillation in EJ-200 Plastic

EJ-200 is one plastic scintillator used by the BYU Nuclear Group's cadmium detectors. The plastic is made from the polymer polyvinyltoluene ($C_{10}H_{11}$) with a few percent organic fluors [9]. The fluors are used to shift light generated in the scintillator and have them peak at 425 nm with a rough distribution in the 400-500 nm range [10]. Fig. 2.4 below shows the distribution of wavelengths emitted from the EJ-200 plastic.

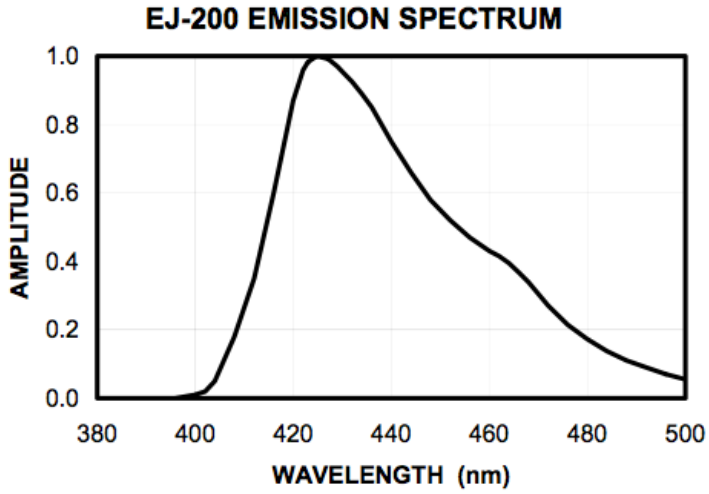

Figure 2.4 Wavelength distribution for EJ-200 plastic scintillator.

For organic scintillators in general, the process of scintillation occurs when, as stated by Turner, "Incident radiation causes electronic excitations of molecules into discrete states, from which they decay by photon emission" [11]. For EJ-200 specifically, the molecules that are excited by incoming protons or electrons are the benzene rings in the plastic. Turner further explains that due to low-Z composition (nucleon number per atom), these organic scintillators are "generally most useful for measuring alpha and beta rays and for detecting fast neutrons through the recoil protons produced."

2.2.2 Scintillation in ^{6}Li-glass Doped with Cerium

^{6}Li-glass, doped with cerium is another scintillating material used by the BYU Nuclear Group. However, unlike the Cd-capture detectors used in the group, which have separate capture and scintillating materials, the ^{6}Li-glass encompasses both pieces–the capture and scintillating materials–in one.

Even though ^{6}Li would technically be considered an inorganic material (i.e. no C or H), because it is in the form of glass (along with the cerium doping), for the process of scintillation we will consider it an "organic" scintillator. When the previously discussed alpha-triton pair is produced in the glass (resulting from neutron capture), these two charged particles proceed to excite the atoms of cerium (via electronic excitation as in the case of regular organic scintillators) also in the glass. The cerium then de-excites by releasing a photon. The same process may occur when a gamma ray causes Compton scattering of an electron in the glass, which electron will also excite the cerium leading to a subsequent photon being released.

Of particular interest in these two separate cases is the size difference (and subsequent mean free path) of the alpha and triton particles as compared to the electron. Because the alpha and triton are much larger, their mean free path is smaller. As a result, they are likely to deposit most of their energy in the glass (some of which goes to cerium excitation) before escaping–if they escape. The electron, however, will have a much larger mean free path. As such, it is likely to deposit less energy in the glass, and, as a result, less energy to the cerium excitation, before it exits the glass. This difference becomes a key used in Pulse Shape Discrimination (PSD), which we will discuss shortly.

2.3 From Light to Electronic Signal

The final step in the conversion of a neutron interaction into a readable electronic signal is the photomultiplier tube (PMT). The PMT is used to gather light output from the scintillation process and turn it into electrical pulses via a 3-step process: (1) photo-electron emission, (2) electron cascade from the electron multiplier stages and finally (3) electron collection at the anode. The explanation to follow comes from Knoll's explanation on the PMT process [7].

After photons are created in the scintillation process, they proceed to the PMT. On the large,

visible inner surface of PMT, including the inner surface of the glass face, there is a thin coating of photocathode material. The photons from scintillation come into contact with the photocathode material, and, if there is enough energy, cause an electron to eject from the material. It is possible that this electron may "bump" into other electrons during the ejection process. There is also an energy difference that exists between vacuum and the photocathode material. In order to eject, the electron must have enough energy to overcome this difference–also known as the work function. The electron, known as a photo-electron as it was ejected by a photon, will then head toward the electron multiplication part of the process.

To multiply the number of electrons resulting from photon incidence on the photocathode, the photoelectrons are accelerated to a series of positively charged plates known as dynodes. The photoelectrons impact material on the first dynode. For each collision, if there is enough kinetic energy, the photoelectron will knock loose multiple electrons. These newly freed electrons will then be accelerated toward the second dynode where they will hopefully each knock loose more electrons. The process continues through mutliple dynodes. After acceleration to and collision with each dynode, the resulting myriad electrons are gathered at the PMT's anode where they are fed as an electronic signal to a waveform digitizer.(This signal may be amplified or attenuated en route to the digitizer.)

In the case where there is no bias voltage on the PMT, photoelectrons in this overall process, according to Knoll, have around 1eV or less kinetic energy once they have left the photocathode. However, once a positive voltage potential is added to the first dynode (and subsequent dynodes), the effective kinetic energy of the photoelectron via Coulomb interaction with the positive dynodes becomes great enough to knock multiple electrons free upon collision with the first dynode. .These newly freed electrons, as stated by Knoll, only have a few eV kinetic energy. They are, however, accelerated by the second dynode's positive potential where they free more electrons upon impact with the process continuting through multiple dynodes.

Chapter 3

^{3}He-, ^{113}Cd- and ^{6}Li-Based Detectors

The mainstay of the BYU Nuclear Group's detector arsenal has been cadmium and lithium: specifically cadmium-113 metal and lithium-6 glass. Both elements provide an alternative to ^{3}He in the realm of neutron detection. Both detector types (Cd- and Li-based) approach neutron detection from a methodology different from that of ^{3}He and different from each other. However, both prove to be effective neutron detectors in their own right.

3.1 ^{3}He-based Neutron Detection

^{3}He has the simplest form of neutron detection methodology. Because ^{3}He is very insensitive to gamma rays, it is not plagued by the issue of misidentifying gamma rays as neutrons. Below you can see the reaction formula:

$$ {}^{3}_{2}He + {}^{1}_{0}n \rightarrow {}^{3}_{1}H + {}^{1}_{1}p \tag{3.1} $$

A ^{3}He detector counts the number of neutron reaction events occurring over a given period of time. In the application of portal monitoring, the recorded flux is then compared to a proscribed

limit. This makes the process from neutron-^{3}He collision, to recording the event in a computer system simple, straightforward and short.

However, as mentioned earlier, ^{3}He is in short supply. Not only this, but modeling done by Lawrence Rees at BYU shows that ^{3}He detectors in their current design become ineffective at detecting neutrons when a neutron source is shielded (i.e. encased in water or plastic) [12]. This stems from the fact that ^{3}He detectors have a higher detection efficiency at lower neutron energies and are already "shielded" by a built-in layer of moderation that is used to slow high-energy neutrons so they can be detected by the ^{3}He. If a source is already shielded, neutrons must not only pass through the initial moderation, but ^{3}He's built-in moderation as well. As a result, this decreases the detector's ability to detect neutrons. Also, though not as likely in Homeland Security application, these detectors, without their built-in moderation are not able to detect higher energy neutrons.

Tomanin *et.al.* conducted a study to optimize the use of ^{3}He in present border detection systems. In essence, they were able to show that the current design/configuration of ^{3}He detectors was not ideal from a ^{3}He consumption perspective and suggested possible alternatives that used more moderation and more tubes but at lower gas pressures [4].

3.2 Cadmium-based Neutron Detection

As discussed previously, the cadmium-based detector is one of the primary detectors used by BYU's Nuclear Group. All though the group has created a variety of detectors based on cadmium, including the Hybrid Detector with which this work is mainly concerned, we will first focus on the general concept.

The general construction of the cadmium-based detector consists of slabs of plastic scintillator with aluminum mylar-cadmium metal-aluminum mylar sandwiches in between slabs. A PMT is

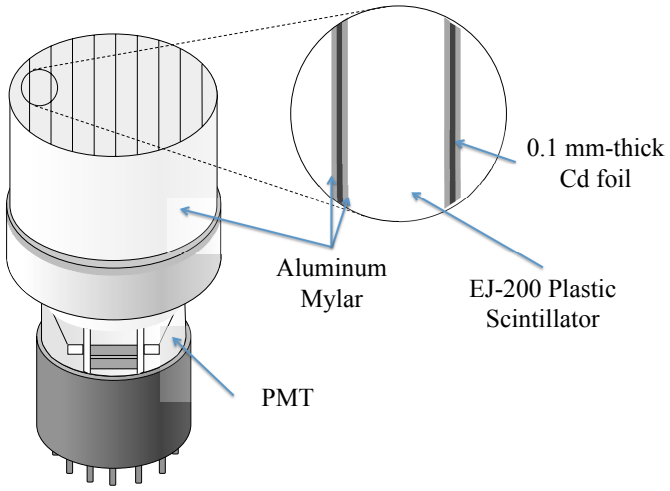

Figure 3.1 General construction of a Cd-based detector as used by the BYU Nuclear Group.

placed on the end of the bulk of slabs, such that it (the PMT) can see each plastic slab. (Fig. 3.1 depicts the general construction of a Cadmium detector.)

Unlike ^{3}He, cadmium-based detectors *are* sensitive to gamma rays. As discussed previously, the process of scintillation in plastic, EJ-200 for example, occurs whenever a charged particle moves in the plastic. The charged particles can be the result of neutron interaction (proton recoil and neutron capture) or gamma-ray interaction (Compton scattering) with the material. When an event–a pulse of light in the scintillator–occurs and is read into the digitizer, it is impossible to tell *a priori* whether the event was triggered by a neutron or gamma-ray. To overcome this challenge, the cadmium-based detection methodology relies on the concept of double pulses.

An ideal neutron event occurring within a cadmium-based detector would follow this process:

1. A neutron enters the cadmium-based detector and most likely collides with a hydrogen nucleus within the plastic.

2. The hydrogen nucleus is dislodged by the collision and moves through the plastic, causing the plastic to scintillate. This results in an electronic signal fed into the computer. This is pulse 1, also known as the recoil pulse.

3. The neutron, having been slowed enough by its collision with the hydrogen nucleus, comes into close proximity to a ^{113}Cd nucleus (in the cadmium metal) and is captured by that nucleus.

4. The nucleus becomes excited and subsequently emits gamma rays.

5. A gamma ray scatters from an electron in one of the atoms in the plastic (Compton scattering). The resultant free electron causes the plastic to once again scintillate, with its subsequent electronic signal being sent to the computer. This is pulse 2, also known as the capture pulse.

When two pulses are within about 16 μs of each other, this is deemed a neutron event. There is no guarantee that any pair of pulses constitutes a neutron event in the detector. There is the possibility that both pulses were gamma ray events that coincidentally occurred within the 16 μs time window. We therefore track the difference in time between pulses as well as require that pulses reach a certain size-threshold. Specifically, we require that at least one pulse must be above the trigger threshold so as to have the event recorded. Other pulses recorded close to the trigger pulse must reach either a pre- or post-trigger threshold, otherwise they are not counted as pulses in the software analysis. By enforcing pulse thresholds, we help to eliminate background noise. Then, by tracking the time difference, we can know with greater and greater confidence that the closer two events are in time, the more likely they are the result of a proton-recoil/neutron-capture pair (a neutron event) vs. two random gamma ray events.

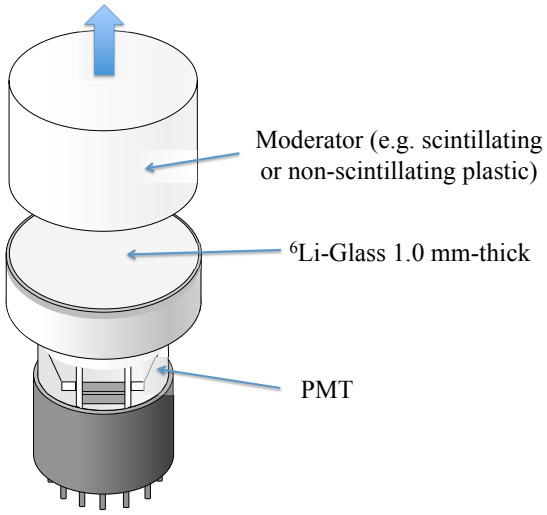

Figure 3.2 Design of Li-glass detector with glass in between moderator and PMT.

3.3 Lithium-Based Detection

The detection methodology of Lithium-glass-based detectors is markedly different from the previous two methodologies. Like cadmium detectors, ^{6}Li-glass detectors *are* sensitive to gamma rays. However, unlike cadmium, ^{6}Li-glass detectors are able to "discriminate" (to a degree) between light output of neutron events vs. gamma ray events.

The general design of a ^{6}Li-glass detector is quite simple. First, it consists of a 1 mm-thick disk of ^{6}Li-glass doped with cerium. The glass can then be arranged into different geometries with a moderating material (e.g. a scintillating or non-scintillating plastic). The desired geometry of glass and moderator will depend on the energy of incident neutrons. If the neutron source is unmoderated, the glass will need to go in between the PMT and plastic so that the plastic can slow the incoming neutrons. If the neutrons have already been moderated, the plastic can go in between the glass and PMT. Here, we will consider the geometry of glass in between plastic and PMT. Fig. 3.2 demonstrates the configuration.

The general process for neutron detection in the ^{6}Li-glass detector:

1. A higher energy neutron enters the plastic moderator and collides with multiple protons until it is slowed enough to allow itself to capture in the ^{6}Li-glass.

2. Once at a low enough energy and in close enough proximity to the ^{6}Li-glass, the neutron is captured by a ^{6}Li nucleus.

3. The ^{6}Li nucleus-neutron capture results in a temporary ^{7}Li nucleus which immediately fissions into an alpha particle and triton.

4. Both the alpha and triton are charged particles that, in the presence of cerium-doped glass, cause the glass to scintillate (see Sec.2.2.2).

5. The alpha-triton pair, resulting from the fissioned lithium, has a mono-energetic combined total energy. For reactions with almost zero neutron energy, the resultant energies for the alpha and triton are, respectively, E_{α}=2.05 MeV and E_{T}=2.73 MeV [7]. Because the mean free path of both the alpha particle and triton are short in comparison to the thickness of the glass, they almost always remain in the glass.

6. The result of the alpha-triton pair scintillation is a pulse of light that is, theoretically, always the same exact size–a feature that can be isolated almost like a neutron "thumb-print".

Depending on the setup, different events will have different pulse characteristics. For a Li detector with glass coupled to EJ-212 "fast plastic", the alpha-triton pair that scintillates in the glass will theoretically always create pulses of the same size (area) and width. In reality there is a slight spread in the size and width of these pulses. Gamma rays that Compton scatter in the glass will tend to create smaller pulses than those of the alpha-triton. They may, however, have similar width ratios as the alpha-triton pairs. If the gamma rays scatter in the plastic, they may be just as large (in area) as the alpha-triton pulses but will tend to be narrower.

In the case where there is no plastic scintillator optically coupled to the PMT and glass (the setup used in the hybrid), the gammas tend to be smaller than the alpha-triton pulses. Their width ratios may be smaller, the same size or larger than those of the alpha-tritons. In general, a majority of the gamma width ratios tend to be of the same size or larger than the alpha-triton width ratios.

These pulse shapes, with the detector setup taken into account, help us to discriminate between neutron and gamma events. In the setup of glass and fast plastic, we will look for events that have a consistent width ratio and area. These are likely to be neutron events. Narrower events are likely to be gamma events. In the case with no plastic, we again look for consistent pulse width ratios and pulse sizes. These are likely to be our neutrons. Smaller pulses will likely be gamma events. Both of these methods provide differing forms of Pulse Shape Discrimination (PSD) as used by members of the BYU Nuclear Group. The second method is used for work on the hybrid detector.

3.4 Results from the Cd Capture-gated Detector

In his senior thesis, working with a Cd-based detector, Nathaniel Hogan [13], in conjunction with the BYU Nuclear group, was able to describe the Δt distribution of a Cd-based detector, very similar in construction to the Cd component of the hybrid. He was also able to determine the detector's intrinsic efficiency–the number of neutron events counted vs. the total neutrons hitting the detector face. In his setup he calculated around 1,174,230 neutrons hitting the detector face in the first as well as second runs. (Each run was 45 min-long with a calculated rate of 434.9 neutrons per second hitting the detector face.) He summarized the total number of doubles (referred to as dual pulse signatures (DPS)), which were then divided into accidental doubles and actual neutron doubles.

To calculate accidental doubles, Hogan classified doubles that occurred further apart in time than 24 μs to be background doubles. Table 3.1, copied from Hogan's thesis, lists his results.

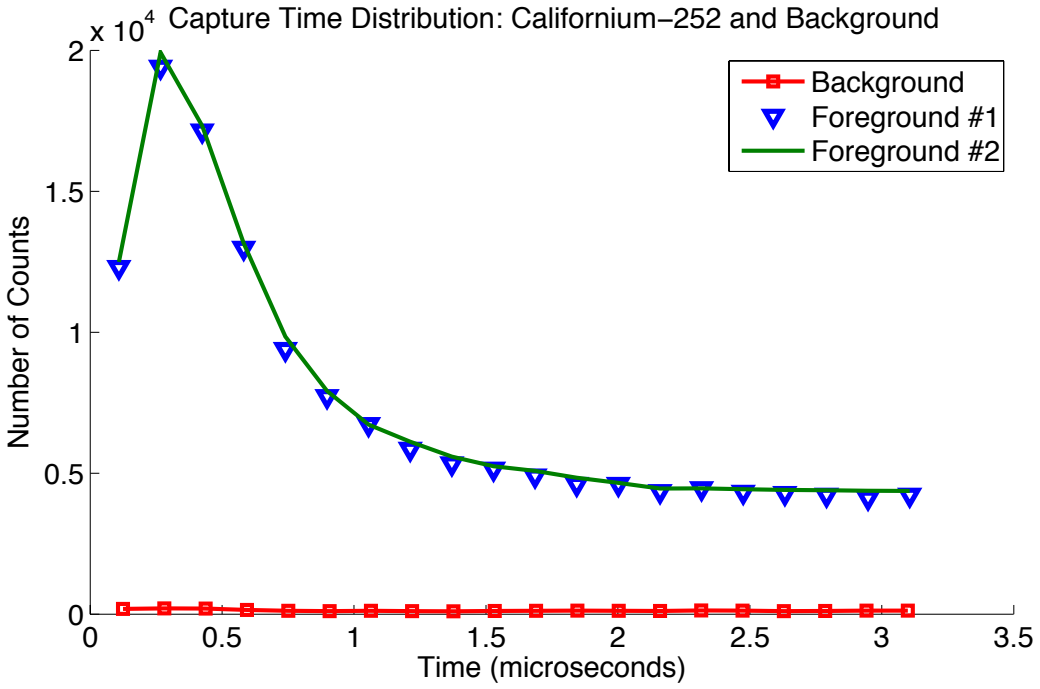

Figure 3.3 Hogan's Cd detector Δt distribution as given by Hogan in his thesis.

Also, a plot from Hogan shows the Δt distribution for his Cd detector for one background and two foreground runs (Fig. 3.3).

Run	Total DPS	Late-time Accidentals	Total Real DPS	Intrinsic Efficiency
Foreground #1	143,587	82,396	61,191	5.21%
Foreground #2	147,241	85,580	61,661	5.25%

Table 3.1 Summary of doubles results and intrinsic efficiency of Hogan's Cd detector, taken from Hogan's thesis.

3.5 Results from the Li-glass Detector

Adam Wallace [14], in his senior thesis work, described the attributes and results of a ^{6}Li-glass detector utilizing a cylinder of plastic scintillator. Specifically, his setup used a 1 mm-thick piece of glass set on a plastic scintillator (both EJ-240 "slow plastic" and EJ-212 "fast plastic" were used, however, the EJ-212 seemed to be emphasized more in his work), with the plastic scintillator coupled to a PMT using optical grease. In this case (which is different from the Li component of the hybrid) both the glass and plastic were optically coupled and both were scintillators.

Wallace found that a Li-based detector with a 4 cm-thick plastic moderator (also acting as a scintillator), in between the glass and PMT, yielded an intrinsic efficiency of 30% when the source was shielded by 10 cm of water. Wallace utilized Pulse Shape Discrimination (PSD) to identify neutron events in the detector. The neutron captures form a "neutron cloud" as the result of capturing the neutrons in the lithium is mono-energetic as a whole. The neutron cloud is demonstrated in Fig. 3.4.

Wallace does state that it is possible for a ^{60}Co source to create events in the cloud as well, but only if all of the energy from Compton scattering of both Co gamma-rays in the glass remains in the glass. Through his work, Wallace shows that 1 in every 10,000 gamma ray events are misidentified as a neutron event. This is shown in the scatter plot of a gamma ray spectrum with a few events that find themselves in the location where the neutron cloud ought to be (see Fig. 3.5).

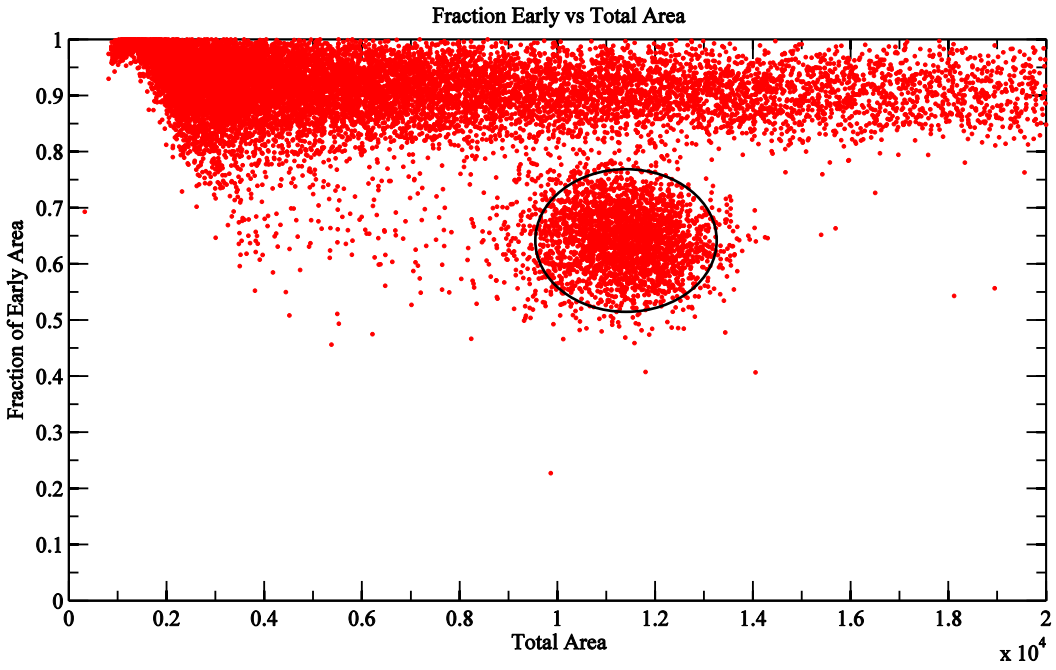

Figure 3.4 Plot taken from Wallace's thesis of a "Neutron Cloud" formed by the mono-energetic reaction of neutrons being captured by ^{6}Li nuclei in the glass. Distinguishing between neutrons and gammas is done using PSD. Run taken using ^{252}Cf.

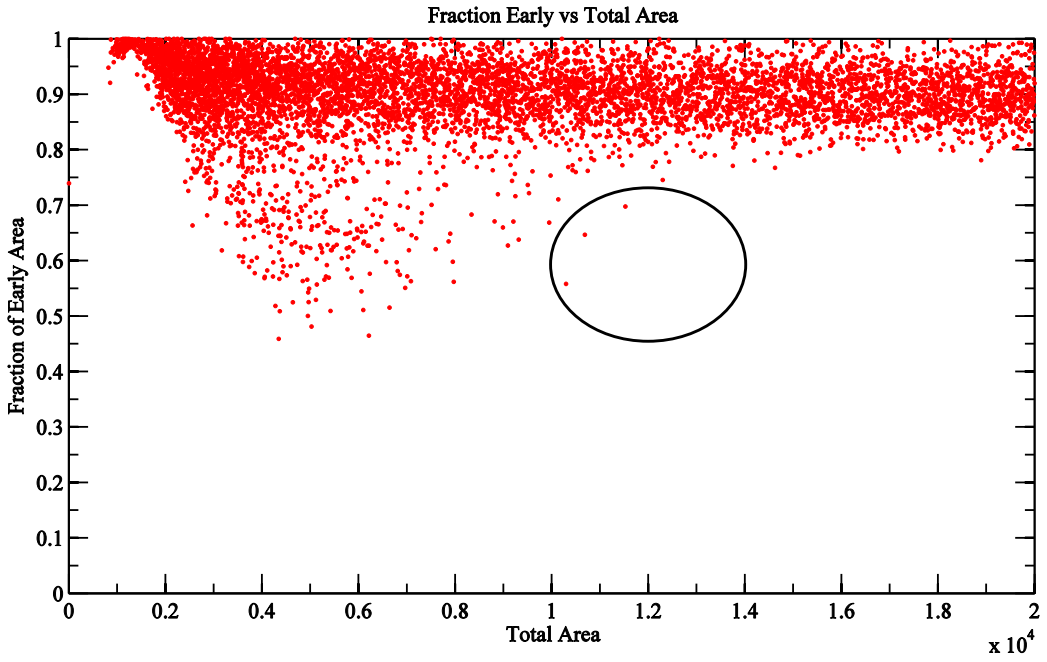

Figure 3.5 Misidentification of gamma events as neutrons within the circle where the neutron cloud "ought" to be. Run taken using ^{60}Co. Plot taken from Wallace's thesis.

3.6 Strengths and Weaknesses of Cd and Li Detectors

The benefits of both the Cadmium-based and the Lithium-based detectors are summarized thus:

1. The cadmium provides a relatively reliable process of identifying neutron events based on double pulses. It is also able to detect neutrons at a relatively broad range of energies.

2. The lithium provides for a reliable method of discrimination between gamma rays and neutrons via PSD. Also, it is able to detect neutrons at lower energies.

However, both detectors have inherent weaknesses as well. In the cadmium detector, the biggest challenge is that there is no other way to discriminate between neutrons and gamma rays apart from the presence of two pulses–recoil and capture–that meet time, trigger and threshold requirements. This, however, does not explicitly guarantee a neutron event.

The lithium detector, in contrast to the cadmium detector, can only detect neutrons at lower energies. It requires the presence of a plastic moderator to slow down high-energy neutrons. The question of detection becomes a matter of geometry: where to put the glass in relation to plastic in order to detect both higher- and lower-energy neutrons.

With these challenges in consideration and in a renewed effort to explore how these components may work together, the construction and testing of the hybrid detector has been re-established. (A hybrid detector was built by MargaRita Hoggan and the BYU Nuclear Group before [15]; however, that detector used only one PMT and both the Cd and Li components were optically coupled.)

Chapter 4

The Hybrid Detector

4.1 Research Premise

The primary purpose for the creation of the hybrid detector is to understand if any further benefit can be synthesized by combining the abilities of Cd and Li. Hopefully the individual weaknesses of each component separately will be mitigated when combined into "one" detector.

The first stage in my experimentation was to see how well each component did separately when combined into one detector assembly. Did each component still behave somewhat as expected of Cd- or Li-based detectors in general?

After each component was analyzed for performance in neutron detection, the next step was to combine, to a degree, the abilities of each component. This had already occurred in a sense that the construction of the detector put each component back to back. This had potentially allowed the Li component to use the plastic in the Cd component (optically isolated from the Li section) as a moderator. Going further, was there event information in one side of the detector that could help fill an information gap for the other side? Also, how did the detector behave as a whole?

4.2 Experimental Setup

To describe the experimental setup, I will break it down into three different sub-sections: (1) the construction of the detector, (2) the electronics setup and (3) the actual execution of the experiment.

4.2.1 Detector Construction

As discussed previously, the hybrid detector can be split up into two main components: the cadmium side and lithium side. The cadmium side is made up slabs of EJ-200 plastic scintillator, aluminum mylar and, of course, sheets of cadmium metal. The plastic slabs are each 5.75 in tall and approx. 1 cm thick. Their widths, however, vary such that they create a roughly cylindrical shape when assembled. This geometry allows for getting a close fit to the circular face of the PMT.

The sheets of cadmium-113 are each just shy of 5.75 in tall and are 0.1 mm thick. The sheets vary in width to somewhat correspond to the varying widths of plastic slabs. Each sheet of cadmium is sandwiched between two pieces of aluminized mylar. Each of these sandwiches is in turn sandwiched between two slabs of EJ-200 plastic. The cylindrical stack of plastic slabs is then encompassed about with another layer of mylar. The purpose of the mylar in each case is to reflect scintillated light back into the plastic where it was created–similar to bumpers at a bowling alley. The detector is capped with a piece of mylar at one end of the cylinder. A PMT is then affixed to the other end using optical grease. (See Fig. 3.1 in Ch. 3 as it depicts the same type of setup described here, with the exception of the mylar cap.)

The lithium side is simpler in construction: it consists of a piece of 1.0 mm-thick ^{6}Li-glass, doped with cerium, fastened to a PMT using optical grease. The glass and front end of the PMT are covered with aluminized mylar. This keeps the glass optically separated from the cadmium component of the detector so that no scintillated light from the Cd side will "spill" over into the Li side. This also helps to "keep in" scintillated light from the glass. See Fig. 4.1 for a diagram of the

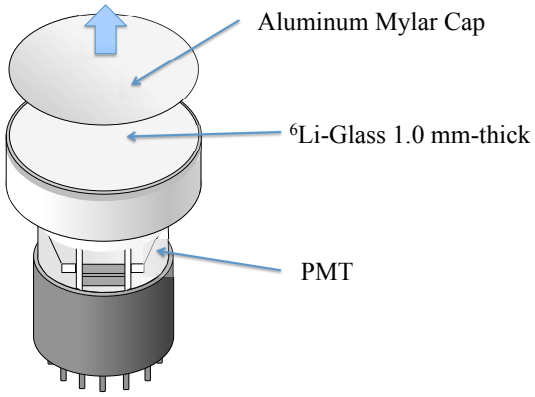

Figure 4.1 Design of Li-glass detector component for the hybrid–no moderator present.

Li side.

Both components–Cd and Li–are then put back-to-back and held together using rubber matting and hose clamps. The figure below illustrates the general construction of the hybrid detector. There are two pieces of mylar shielding each side from the other: the mylar cap on the Cd side and the mylar cap on the Li side.

4.2.2 Electronics Setup

The process of electronic signaling in this setup includes creation of the signal in the PMT, amplification of the signal in a signal amplifier, attenuation of the signal via attenuators, in/out processing of the signal through a desktop digitizer and output to a computer controller interface.

The first step is the conversion of light to an electric signal in the PMT. This detector is equipped with two 5-inch Adit PMTs fixed at either end of the detector. The electrical signals (two separate signals–one from each tube) travel via a BNC cable to two different signal amplifiers. The am-

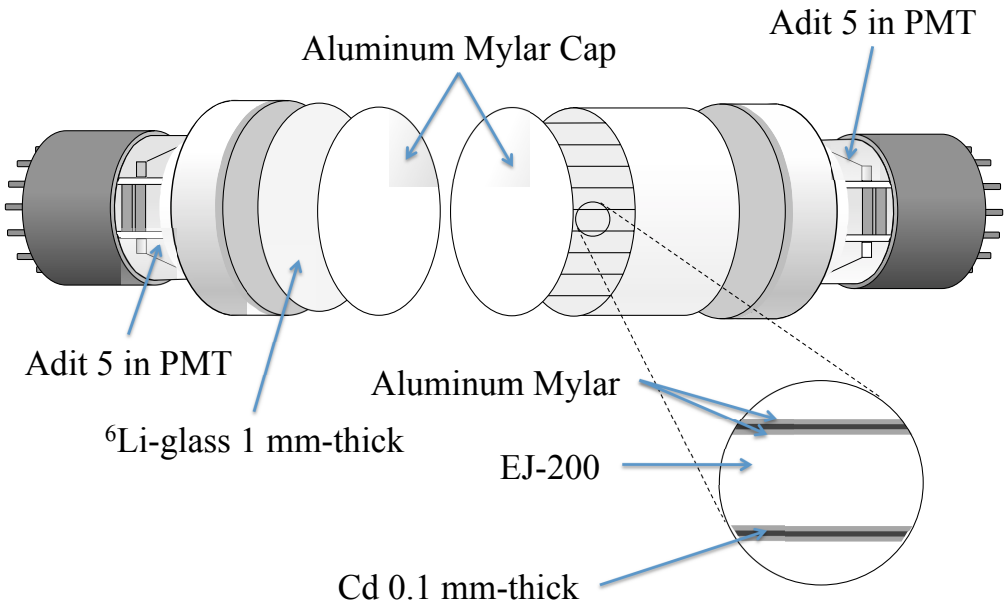

Figure 4.2 Design of entire hybrid detector including both Li and Cd components.

plifiers are set to amplify both signals as follows: coarse gain at 4.0x and fine gain at 4.5x. Each signal exits its respective amplifier where it is then attenuated by 9 dB before continuing on into a CAEN desktop digitizer. Upon arrival at the digitizer, the signal from the Li-glass side is fed into Channel 0 and the signal from the Cd side is fed into Channel 1.

The digitizer takes both signals, digitizes them and sends the output via a USB cable to a computer running a BYU-created digitizer controller–a software application coded to interface with the digitizer. Once read into the computer, the data are stored as a .dat file in a user-specified folder.

4.2.3 General Experimental Execution

The current setup and execution for data collection with the hybrid detector occurs in a dark box found in the underground research lab. This allows for the detector to be housed in an environment free from external light sources that would otherwise "contaminate" scintillated light and give the PMT a false signal.

One obvious shortfall of the setup is the proximity of the detector to the cement floor. Being approximately 40 cm off the ground means neutrons that initially miss the detector have a higher probability of bouncing back into the detector after hitting the ground than if the detector were further off the ground. The BYU Nuclear Group is currently undergoing tests to help establish at what distance above ground a detector is significantly affected by this neutron reflection known as room return.

4.2.4 Experimental Setup and Execution for Li Side

Before taking data with both channels active and recording, I looked at each component separately first to see how each side of the detector performed on its alone (while still part of the larger detector assembly). I began with the Li side. The Li side took some work to get a good signal.

One setup that ended up working utilized an 88.96 μCi ^{252}Cf source (ref. date 1 Aug 12), known as the "strong source", in the dark box with the detector, approximately 46 cm from the lithium glass face. The source had a Pb brick directly in front of it. The brick was about 4 cm thick. This brick was used to stop many of the gamma rays emanating from the source from getting into the detector. In this way, I could see the neutron and fission gamma spectrum and not worry as much about extraneous gamma rays directly from the source. The source was also surrounded by paraffin wax to help moderate high-energy neutrons so they could be captured in the lithium glass. The detector was then turned on with the lithium glass's PMT (PMT 1) plugged into channel 0 on the digitizer.

Note: During the runs just looking at Li-glass by itself, a 5-in diameter and a 3-cm diameter piece of glass were each used. Both glass pieces were 1 mm thick. Their respective results are discussed subsequently.

4.2.5 Experimental Setup and Execution for Cd Side

The Cd side was similar to the Li side. It took some effort to get results that were meaningful. In the end, when looking at the Cd side by itself I used a 23.76 μCi ^{252}Cf source (ref. date 15 Apr 08)–known as the "weak source". This source was put in the box with the detector, the source positioned on the Li side of the detector approx. 46 cm from the Li-glass (horizontal distance). No moderation or Pb bricks were used in this case. The detector was turned on with the Cd's PMT (PMT 2) being plugged into channel 0 on the digitizer. Channel 0 was used every time each side was being observed individually.

4.2.6 Experimental Setup and Execution for the Entire Hybrid

Not only did I look at individual components (Cd and Li), I also looked at the hybrid detector as a whole. Several configurations with both the stronger and weaker ^{252}Cf sources were used. The

results, which I will outline later, used the following configurations:

- The weak Cf source was placed in the dark box on the Li side (such that source radiation flux passes through Li-glass first) with a Pb brick placed in front and surrounded by paraffin wax. The source was roughly 46 cm horizontally from Li-glass. (All measurements are roughly done on the horizontal, all though the next measurement does include a "bend" in the measuring tape.)

- The weak Cf source was placed in the dark box on the Cd side (such that source radiation flux passes through Cd component first) with no moderation or Pb brick. The source was roughly 41-42 cm from the Li-glass.

- Both weak and strong Cf sources were used. The weak source was roughly 13 cm (horizontal) from corner of dark box, on a cement brick, very roughly in line with main detector axis. The strong source was located on a cart with a Pb brick in front and surrounded by paraffin wax. The front edge of the cart was roughly 1 m (horizontal) from the same corner of the dark box as referenced by the weak source. The resulting distance from Li-glass to weak source ranged roughly from 76-78 cm. For the strong source, the distance ranged roughly from 173.5-176 cm (horizontal distance–vertical distance weren't taken into account).

Chapter 5

Results and Conclusions

5.1 Results

5.1.1 Li Side

When working with ^{6}Li glass as a neutron detector, the key signature of a neutron source (in this case ^{252}Cf) is the neutron "cloud" seen in the PSD plot shown below. This cloud is an intrinsic property of the Li-glass detector and is the result Pulse Shape Discrimination (PSD) in neutron detection. PSD, as used by BYU's Nuclear Group, relies on two variables: the total area of a scintillated light pulse and the width of that same pulse. From the pulse's front edge (marked at a specific channel), we go forward a designated number of channels and set our dividing line. We then analyze the pulse's area before and after the line. Early area is the area before the dividing line. In the scatter plot below, the x component is the total pulse area, whereas the y component is the fraction of early area to the total area.

In the case where there is no scintillating moderator optically coupled to the Li-glass, a majority of the fission gamma events result in scintillation pulses with relativley smaller pulse areas and as such these pulses congregate to the left side of the plot. The neutron capture, however, results in

a alpha-triton pair that is mono-energetic, meaning the pulse size for this capture will generally be the same size for all neutron capture events. This same size pulse is what creates the "neutron cloud" in the scatter plot. Though a few fission gammas may also be found in this neutron cloud, from a Homeland Security perspective, these gammas will not be present. The likeliest spectrum to be seen will be a spectrum of gammas akin to a ^{60}Co spectrum. The figure below (Fig. 5.1) shows the scatter plot for the desired "neutron fingerprint" with a ^{252}Cf source–including both the gamma tail and the neutron cloud. Also, there is a plot of a ^{60}Co spectrum for comparison (Fig. 5.2). Notice that the bulk of the ^{60}Co spectrum tail dies out just before the neutron cloud seen in the ^{252}Cf. There are, however some events that do spill over into the neutron cloud. For these runs, a 3 cm-diameter disk of lithium glass (1 mm thick, doped with cerium), roughly centered on the PMT face, was used. Both runs were approx. 5 min.

Originally, a 5 in-diameter piece of lithium glass was affixed to PMT 1 using optical grease. However, once a good run was taken with the strong Cf source (88.96 μCi), we got a result that had the neutron cloud smeared out, almost in a heart-shape. (See Fig. 5.3.)

This result, was likely due to the PMT. Because the lithium glass is put right on PMT 1, there is no chance for the light to evenly disperse throughout a moderator and uniformly light up the PMT. Instead, the scintillation light occurs only on a part of the PMT–at least most strongly at one point. Depending on the efficiency of the PMT at that point, it may or may not effectively transform the light pulse of a given size into the correspondingly "correct" size of electronic signal. This results in similar-size light pulses (i.e. the mono-energetic alpha-triton pairs from neutron capture) showing up as different sizes (different clouds) because they hit different hot or cold spots on the PMT.

This was corrected by replacing the 5 in-diameter glass with smaller pieces of glass. Using a smaller piece of glass will obviously decrease the efficiency of the Li detector, but it helps to ensure that scintillated light all goes to one area of the PMT such that similar size light pulses produce

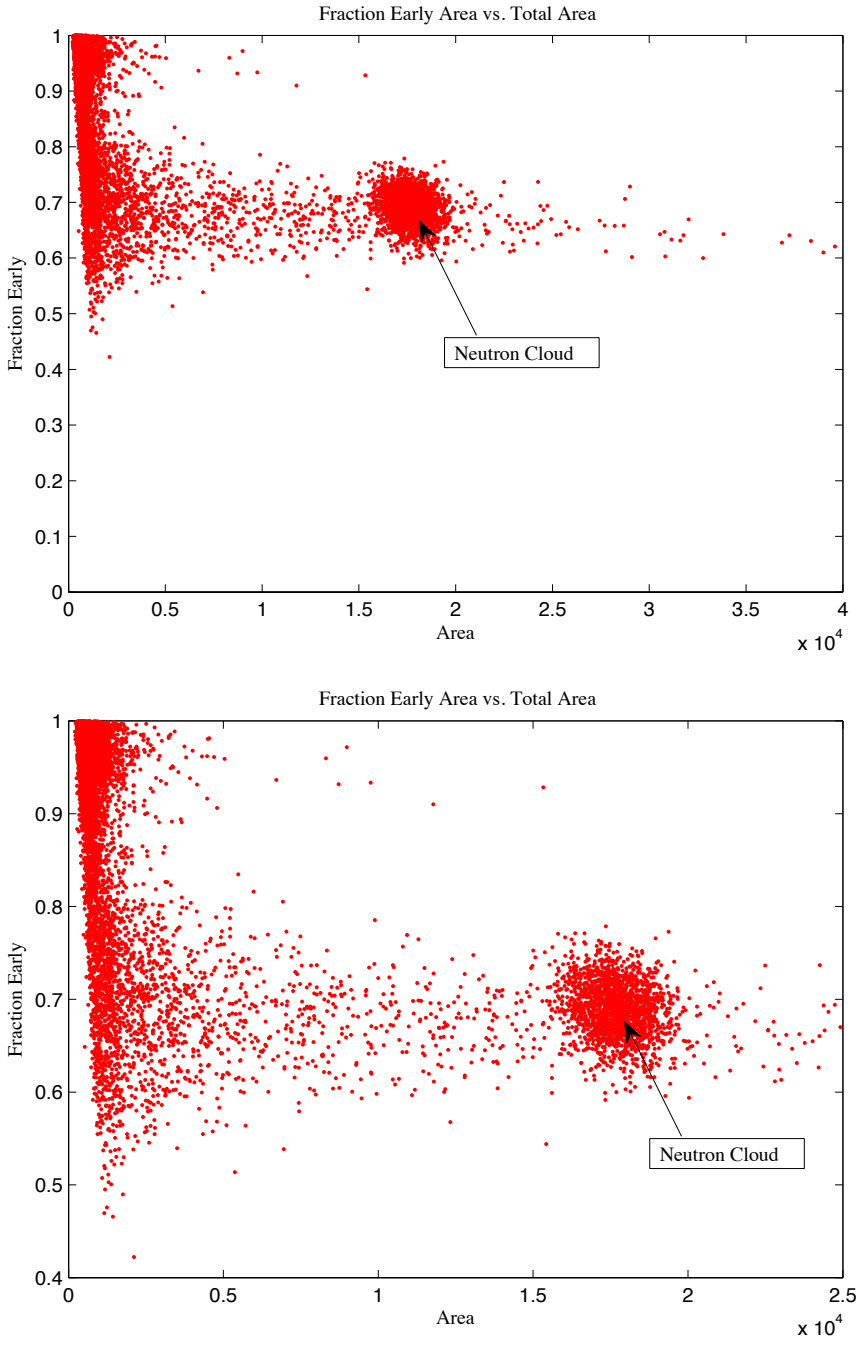

Figure 5.1 The top plot shows a 5 min run from the Li component of detector using a strong (88.96 μCi) ^{252}Cf source. Note the presence of the neutron cloud. The bottom plot shows a zoomed-in version of the top plot.

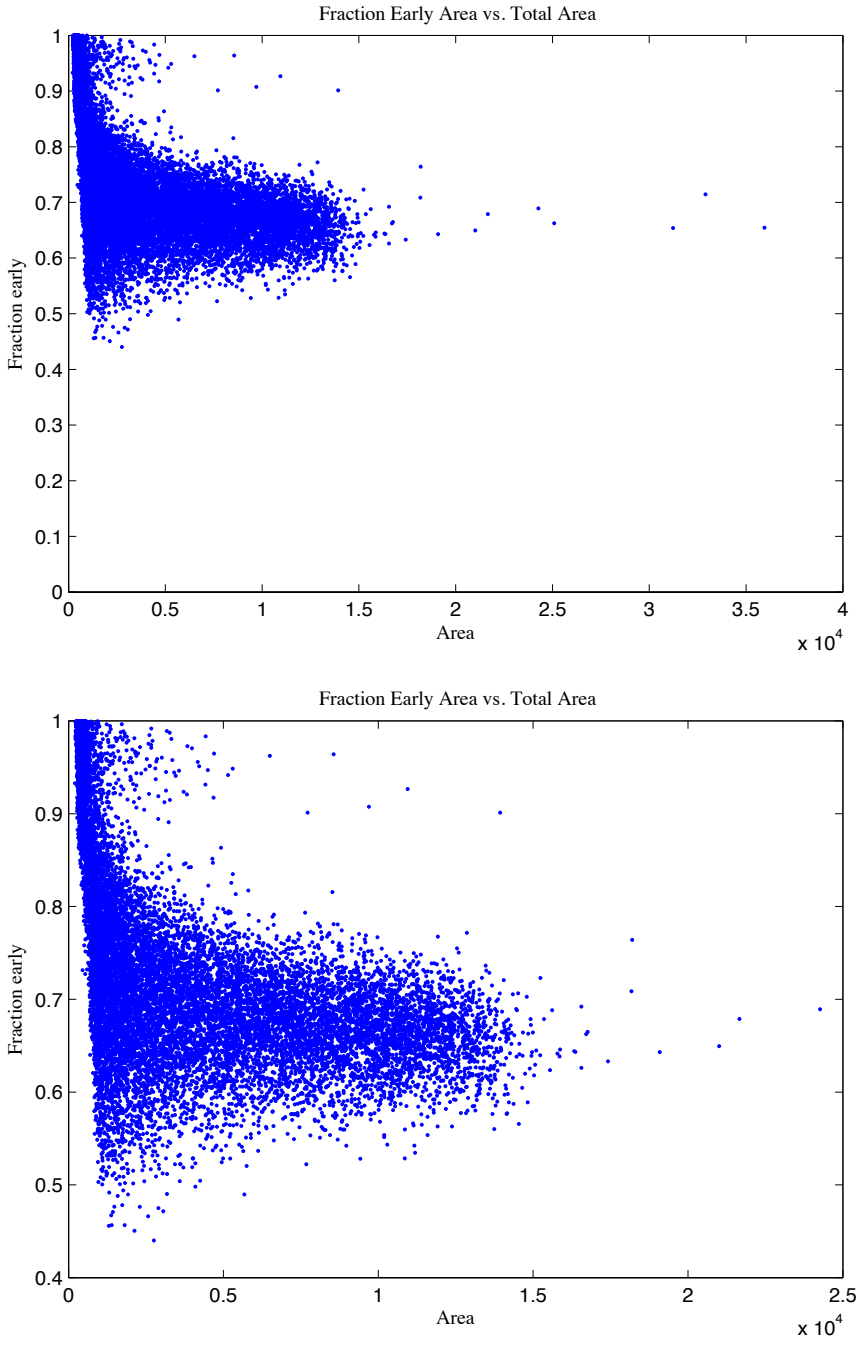

Figure 5.2 These plots show the gamma spectrum when comparing fraction early area vs. total area. The bottom plot is just a zoomed-in version of the top. This was done using the Li component of the detector looking at ^{60}Co. The run was 5 min long.

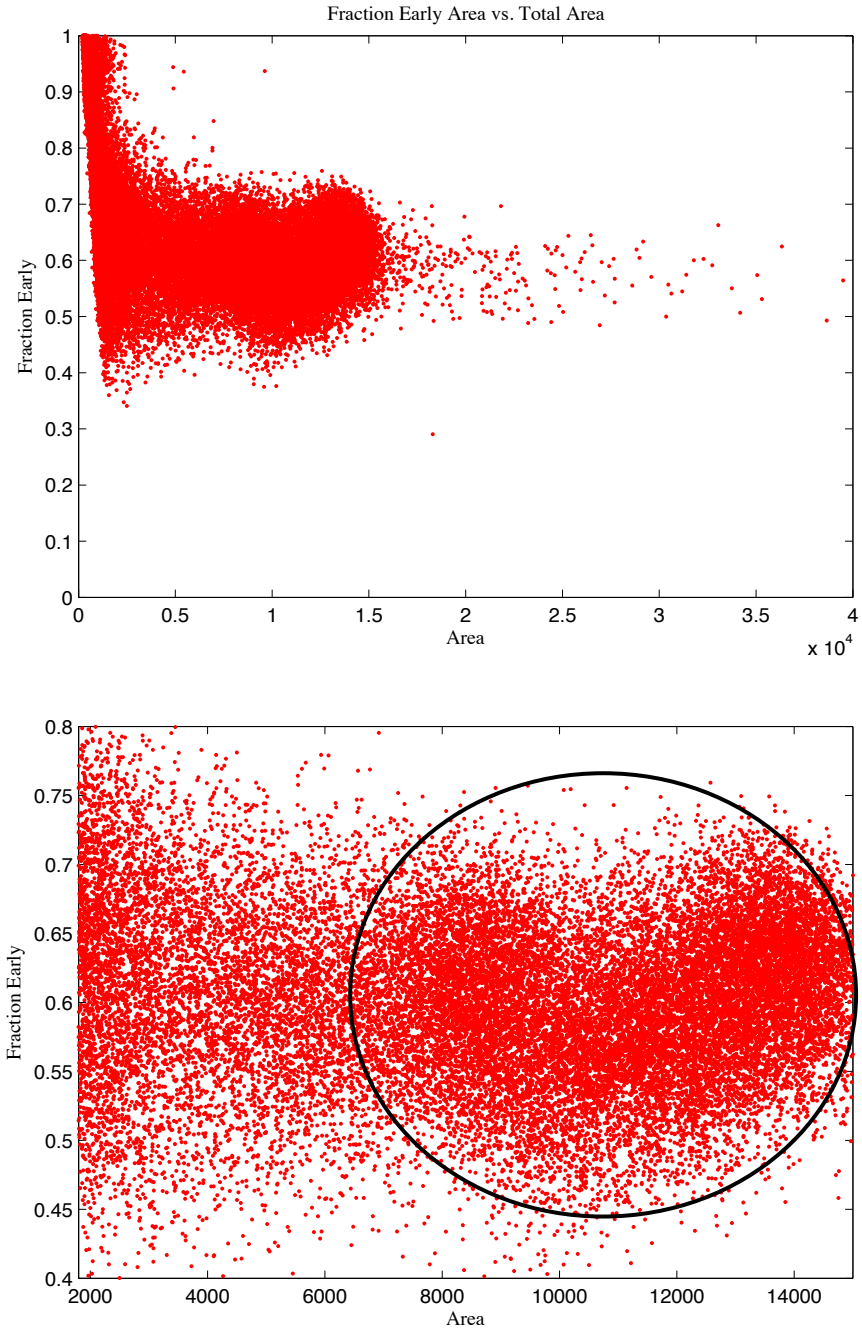

Figure 5.3 Plots (the second being a zoomed-in version of the first) of a 5 min run with strong Cf source using the Li component. Note the neutron cloud is not as consolidated as that of the 3 cm glass used in Fig. 5.1

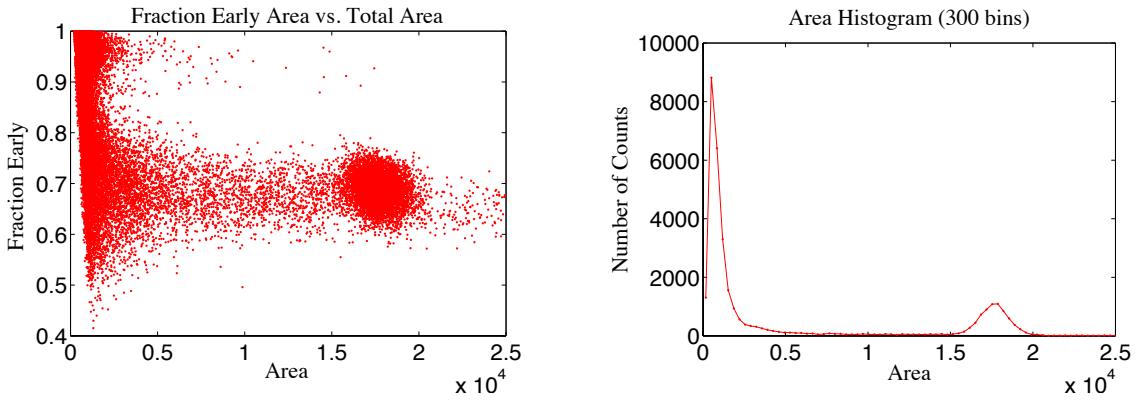

Figure 5.4 20 min run on Li side with strong Cf source. The first plot is the familiar scatter plot. The second is an area histogram. The 3 cm piece of glass was used.

more consistent-sized electronic pulses, albeit perhaps not as strong if the glass is put on a "cold" spot. 3 different smaller-size glass pieces were used during the experiment. In Fig. 5.4, a 3 cm piece of Li-glass was centered on PMT 1. The fraction early vs. total area scatter plot, as well as an area histogram of the 3 cm glass with the moderated strong Cf source, can be seen.

5.1.2 Cd Side

Similar to the Li side, the Cd side required some work to ensure that we were seeing the expected spectrum of neutrons. One of the overall challenges is to ensure that we are not just looking at background radiation (gammas and cosmic ray neutrons). We must also, however, ensure that we are not flooding the detector with such a high neutron flux such that the digitizer gets bogged down and data is lost. One key aspect to distinguishing between just background radiation and detecting a neutron source, is looking at the time difference distribution between first and second pulses.

For Cd detectors, the principle of double pulses is the key aspect to successful neutron detection. Proton recoil and neutron capture events (pulses 1 and 2) are more likely to occur closer together in time. As such, a plot of the time difference (Δt) distribution would show a large number of events with small Δt and fewer events with increasingly larger Δt: the distribution will look

similar to an exponential decay function. Random background, however (especially since it will consist of random gamma ray events) will produce a Δt distribution that will just look like noise. That is, the Cd detector is prejudiced toward small Δt. If two pulses occurred within a small period of time (say within 16 μs or less), it is more likely that the two constitute a proton recoil/neutron capture pair, whereas two events further away in time, are more likely to be two random gamma events, etc.

Fig. 5.5 shows the Δt distribution–again this idea that neutron events detected in the Cd side will be biased toward smaller Δt. It also shows a plot of area and peak height distributions.

5.1.3 The Hybrid as a Whole

General Results

First, the hope for the hybrid detector was the ability to simply combine the skill set of Cd and Li-based detectors into one detector– the benefit being able to detect neutrons over a wider energy range. The Cd side would cover higher energy neutrons and the Li side would detect lower energy neutrons. Secondly, there is the additional question of whether or not any information in one side of the detector can aid, or in our case, act as a second confirmation of a neutron event. This is discussed specifically later on when we look to see if a single proton recoil pulse in the Cd side corresponds to any capture events in the Li side. But first, we'll backtrack to see how the hybrid did as a whole.

All in all, regardless of the source setup used (as outlined in 4.2.6), most events were seen in the Cd side of the detector. The Li side was given a trigger of -200 mV. This was meant to help eliminate a lot of the gamma-noise that would otherwise be present, while still giving room enough to see the neutron cloud should it occur. The Cd trigger was set at -60 mV or -75 mV depending on the run.

Plots for the Li side and corresponding Cd side are seen in Figs. 5.6-5.9. Note here that the Li

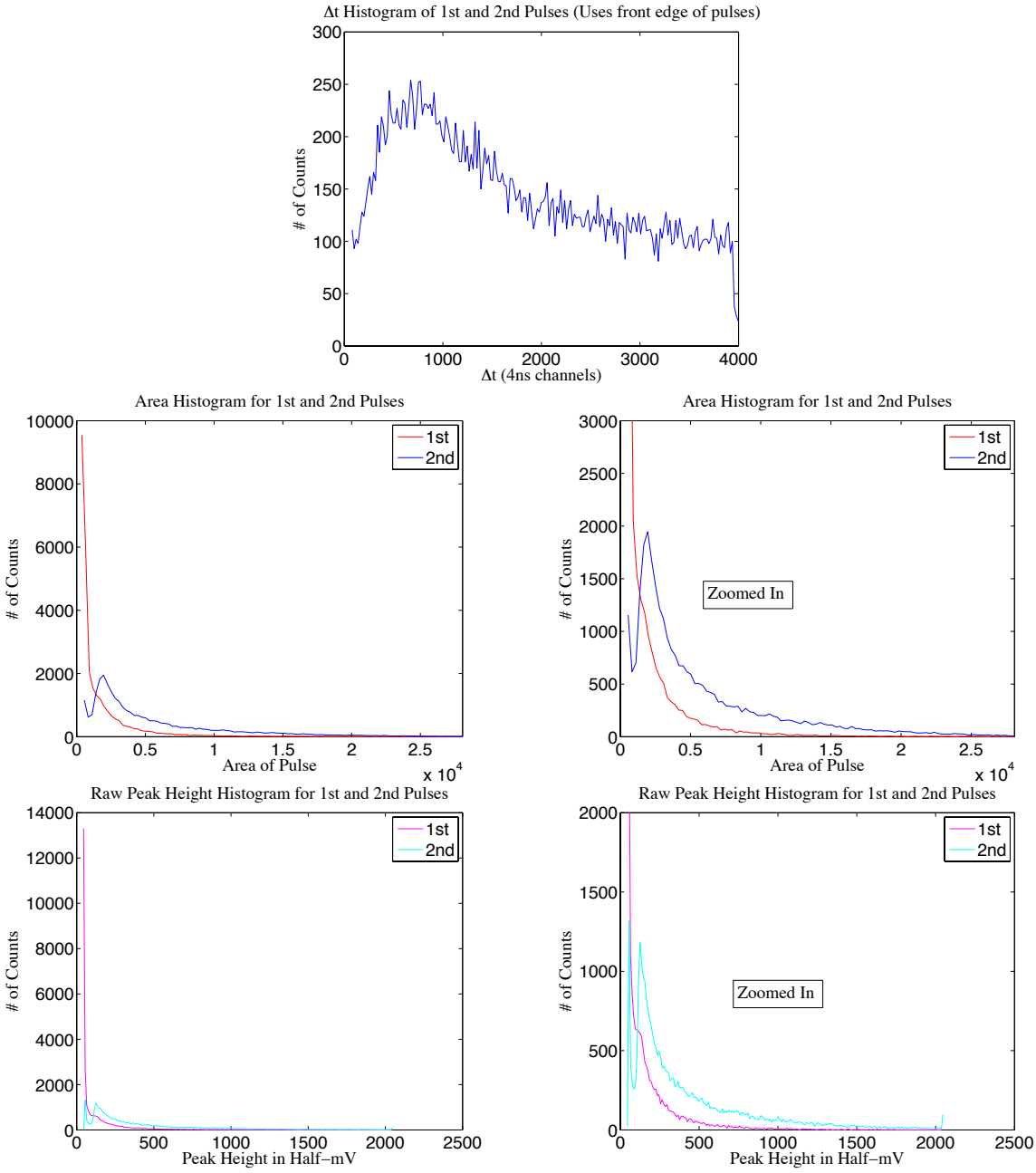

Figure 5.5 Δt, area histogram (including zoomed-in version), raw peak height histogram (including zoomed-in version) plots for Cd component. The run was taken for 30 min using the weak Cf source, positioned on the Li side of the detector, roughly 46 cm from the glass.

side has very few events (little or no neutron cloud) whereas the Cd side looks similar to what was seen when we looked at the detector with only the Cd side turned on. For the first 3 runs shown here, a roughly 1 in-diameter piece of Li-glass (2 mm-thick) was used. This piece was not either the same 3 cm nor 5 in pieces use during the runs looking at the Li side by itself. The last run shown uses a piece of Li-glass shaped similar to a cat eye slit (approx. 8.5 cm long, 2.75 cm wide and 1 mm thick) roughly centered on the PMT. Also, for the last run shown, a piece of moderating plastic, 5 in-diameter and 9 mm-thick, was put in between the Cd and Li side of the detector. Both sides still remained optically isolated from each other and the plastic.

Table 5.1 illustrates different aspects (doubles, triples, combos, etc.) from each of the runs.

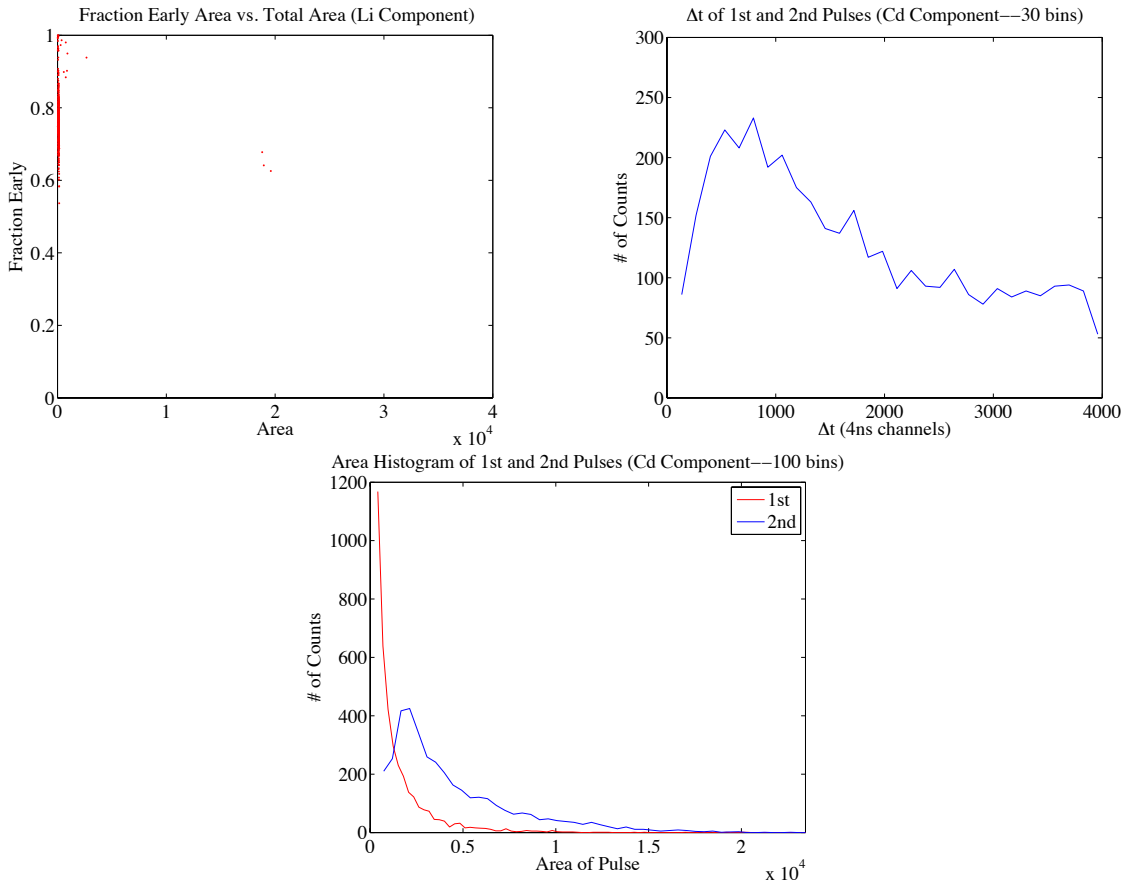

Figure 5.6 Fraction early vs. total area for Li side–Δt and area histogram for Cd side; The run was taken for 20 min using the weak (23.76 μCi) ^{252}Cf source. The source was placed on the Li side, roughly 46 cm from the glass. The source had a Pb brick in front of it and was surrounded by moderator. (12Apr14)

Using Cd Single as Double Confirmation for Neutron capture in Li

One point of interest with this detector was to see if there would be any proton recoil events that would then result with a capture in the Li-glass. With Cd-capture methodology, singles are thrown out as it is impossible to tell whether the events were neutron or gamma-triggered. Is it then possible to recoup some of those lost events by seeing their capture pulses in the lithium?

Unfortunately, this was not the case. In the software analysis, conditions were setup to make a count of all of the incoming events where there was first a single in the Cd side and then a capture in

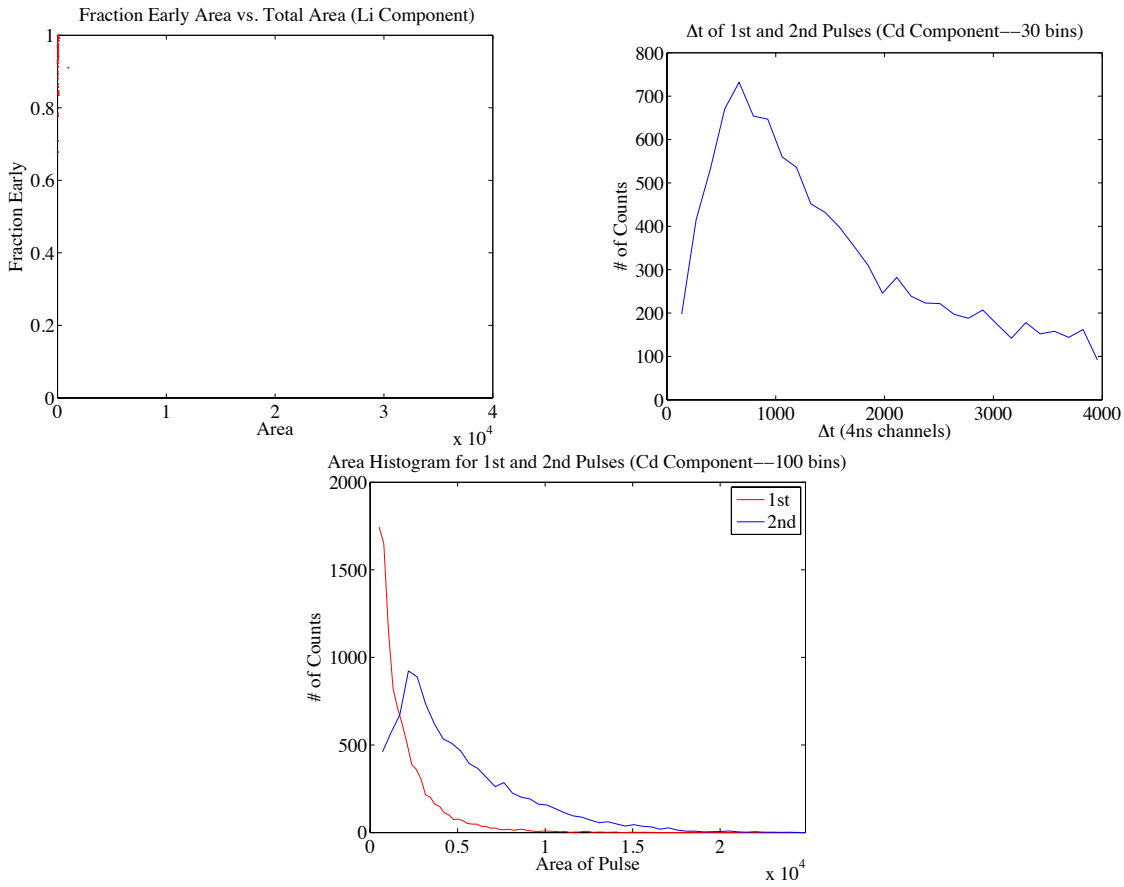

Figure 5.7 Fraction early vs. total area for Li side–Δt and area histogram for Cd side; The run was taken for 10 min using the weak (23.76 μCi) ^{252}Cf source. The source was placed on the Cd side, roughly 41-42 cm from the Li-glass. There was no Pb brick nor moderator. (14Apr14)

the Li side (pulse area between 1.5x10^4 and 2.5x10^4), both events within 16 μs of each other–with the Cd pulse obviously being first. Very few events met this requirement (< 0.1%). See Table 5.1 for percentages on Cd proton recoil/Li capture "combo" events.

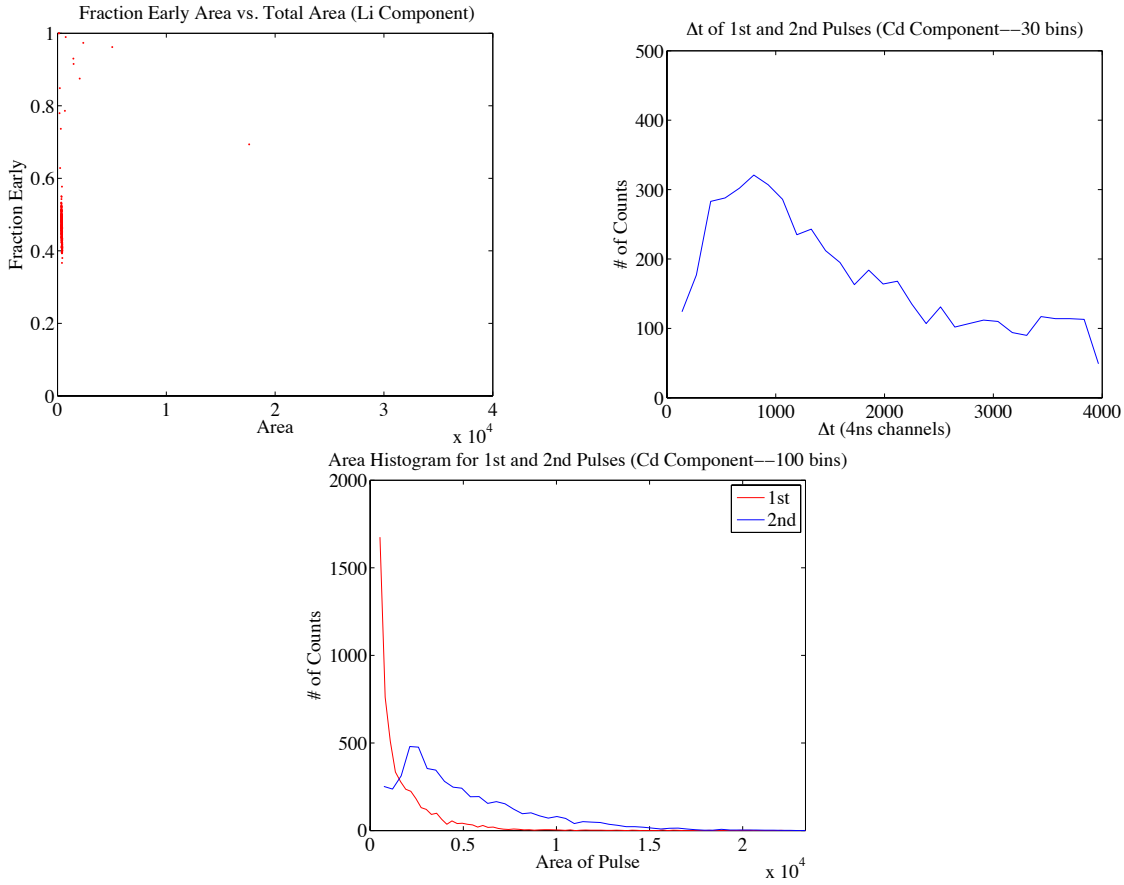

Figure 5.8 Fraction early vs. total area for Li side–Δt and area histogram for Cd side; The run was taken for 15 min using both the weak (23.76 μCi) and strong (88.96 μCi) ^{252}Cf sources. The sources were placed outside the dark box, at different distances, very roughly in line with the main axis of the detector assembly. (15Apr14)

5.2 Conclusions

5.2.1 As Two Separate Detectors

As separate detectors, both the Li and Cd components both perform well. The Li component, depending on the size glass used, yields a very nice neutron cloud in the scatter plot of fraction early vs. total area. It is also possible to see the cloud as a solitary peak in a corresponding area histogram. Especially because there is no plastic scintillator present, the only events that really have the right peak height and pulse area (with the exception of some of the fission gammas from

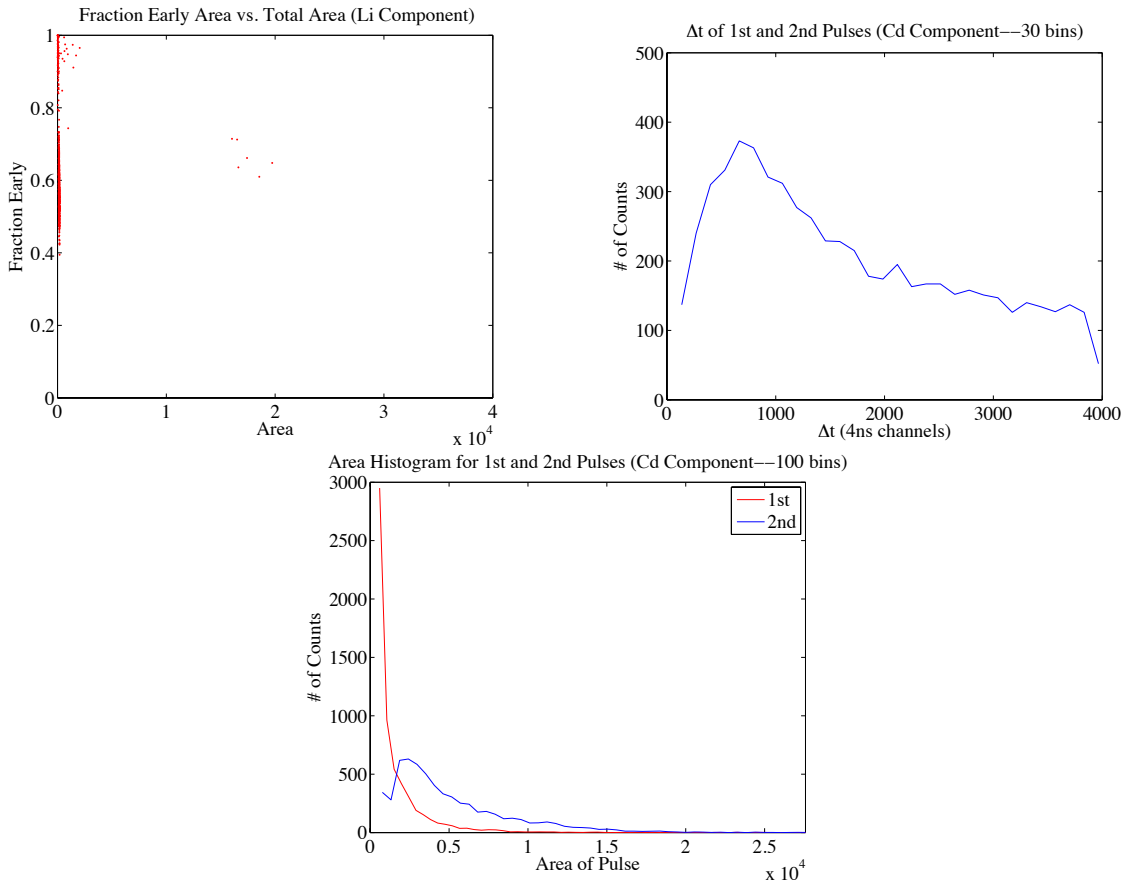

Figure 5.9 Fraction early vs. total area for Li side–Δt and area histogram for Cd side; The run was taken for 15 min using both the weak (23.76 μCi) and strong (88.96 μCi) ^{252}Cf sources. The sources were placed outside the dark box, at different distances, very roughly in line with the main axis of the detector assembly. The "cat-eye" shaped glass was used in place of the 1 in-diameter (2 mm-thick) piece of glass. (16Apr14)

the Cf) are the neutron capture events in the Li.

The Cd component also performed well. From the results, we see the Δt distribution follows a rough exponential decay, helping to further substantiate that the Cd detector is prejudiced to smaller Δt's. In essence, the shorter the time between recoil and capture pulses, the likelier it is to be a neutron event.

Description	Tot Events	% Doubles	% Singles	% Triples	% Combos
Weak front; w/ mod	150,730	2.83	94.7	0.0186	0.00730
Weak back; no mod	138,055	7.53	91.1	0.127	0.0138
Both front; strong mod	132,986	4.16	93.7	0.0451	0.0233
Both front; strong mod; "Cat-Eye"	137,686	4.78	92.7	0.0574	0.0225

Table 5.1 Summary of Cd component results including Cd-Li combo events from entire hybrid running at once.

5.2.2 As One Overall Detector

When taken in its entirety, with the setups used here, the hybrid behaves mostly like a Cd-based detector. That is, nearly all of the events occurred in the Cd side of the detector. There were not a lot of Li capture events as attested to by the lack of neutron cloud in the scatter plot. It could be that the runs needed to be better matched in time and setup, i.e. better mimicking the setup of the solo Li run with the moderated strong source in the front corner. However, a run similar to this was done but led to a situation where it probably flooded the digitizer with too many events, causing a potential data loss from the digitizer.

Also, as seen from the previous section, the percentage of Cd-Li combo events was very small. In speaking with Dr. Rees, one possibility to help boost the number of events seen in the Li side would be to increase the intermediary moderation between Cd and Li sides. This would help more neutrons bounce back into the Li side instead of being caught in the Cd side.

5.3 Future

This subject has by no means been exhausted. There is much work yet to be done. First and foremost, work should be done to validate the results given thus far. Some of the runs mentioned

were only 10 or 15 min-long. The runs outlined in Table 5.1 had around 150,000 events or less. Longer runs using the same setup and design should be accomplished to confirm these results.

If and when these results are confirmed, there are still several places to both improve and explore. As alluded to earlier, there is the possibility of exploring the effects of a larger intermediary moderator between components and seeing if this aids in getting more events to occur in the Li side. There is also the issue of exploring different size glass pieces. The larger glass piece (5 in) couldn't resolve the neutron cloud as well as the smaller pieces (3 cm and 1 in). However, the larger piece will have the ability to capture more neutrons due to its larger area.

The analysis program itself could be revisited as well. When looking at raw doubles plots–raw data plots of what the program deemed to be neutron events in the Cd side (doubles)–there would occasionally be a single peak that would be counted as a double. There were also a few triples being counted on this rough pass as doubles. Additionally there were a few occurrences of saturating pulses. One way to counter triples is ensuring the pre- and post-trigger thresholds are set so as to maximize the number of counted doubles and minimize the number of triples gathered from larger background noise. To correct for too many saturating pulses, changes can be made to hardware settings, such as amplification and attenuation. The software analysis program should also be reviewed to ensure any bad events with the above characteristics (2-for-1's, triples and saturating pulses) are minimized then the remainder thrown out.

Overall, there is still much that can be done to explore the abilities and the possibilities of the dual PMT lithium-cadmium hybrid detector.

Bibliography

[1] D. Morgan and D. A. Shea, "The helium-3 shortage: supply, demand, and options for Congress," Congressional Research Service R41419 (2010).

[2] R. T. Kouzes, J. H. Ely, L. E. Erikson, W. J. Kernan, A. T. Lintereur, E. R. Siciliano, D. L. Stephens, D. C. Stromswold, R. M. V. Ginhoven, and M. L. Woodring, "Neutron detection alternatives to ^{3}He for national security applications," Nuclear Instruments and Methods in Physics Research A **623,** 1035–1045 (2010).

[3] R. Kouzes, "Neutron and gamma ray detection for border security applications," In *Proceedings of the 1st International Nuclear and Renewable Energy Conference (INREC10, Amman, Jordan, March 21-24, 2010)*, (2010).

[4] A. Tomanin, P. Peerani, and G. Janssens-Maenhout, "On the optimisation of the use of ^{3}He in radiation portal monitors," Nuclear Instruments and Methods in Physics Research Section A: Accelerators, Spectrometers, Detectors and Associated Equipment **700,** 81–85 (2013).

[5] "DNDO: He-3 shortage not affecting near-term RPM deployments but changes ahead," Terror Response Technology Report 6 (2010).

[6] R. T. Kouzes, J. H. Ely, A. T. Lintereur, E. K. Mace, D. L. Stephens, and M. L. Woodring, "Neutron detection gamma ray sensitivity criteria," Nuclear Instruments and Methods in Physics Research A **654,** 412–416 (2011).

[7] G. F. Knoll, in *Radiation Detection and Measurement*, 3rd ed., R. Factor, ed., (John Wiley Sons, Inc., Hoboken, NJ, 2000).

[8] K. S. Krane, in *Modern Physics*, 3rd ed., S. Johnson, ed., (John Wiley Sons, Inc., Hoboken, NJ, 2012).

[9] E. TECHNOLOGY, "Material Safety Data Sheet: EJ-200 Plastic Scintillator," http://www.eljentechnology.com/images/stories/Data_Sheets/MSDS/200msd.pdf (Accessed April 10, 2014).

[10] E. TECHNOLOGY, "EJ-200 PLASTIC SCINTILLATOR (Data Sheet)," http://www.eljentechnology.com/images/stories/Data_Sheets/Plastic_Scintillators/EJ200"%"20data"%"20sheet.pdf (Accessed April 10, 2014).

[11] J. E. Turner, *Atoms, Radiation, and Radiation Protection*, 3rd ed. (Wiley-VCH Verlag GmbH Co., Weinheim, Germany, 2007).

[12] L. B. Rees and J. B. Czirr, "Optimizing moderation of He-3 neutron detectors for shielded fission sources," Nuclear Instruments and Methods in Physics Research A **691,** 72–80 (2012).

[13] N. Hogan, "Characterization of a Cadmium Capture-gated Neutron Spectrometer," Senior Thesis (Brigham Young University, Provo, UT, 2011).

[14] A. Wallace, "Lithium-Glass Neutron Detection," Senior Thesis (Brigham Young University, Provo, UT, 2011).

[15] M. Hoggan, "Cadmium Capture-Gated Neutron Detector with 6Li-Glass," Senior Thesis (Brigham Young University, Provo, UT, 2011).